European Journal of Medicinal Chemistry 161 (2019) 323–333

Contents lists available at ScienceDirect

European Journal of Medicinal Chemistry

journal homepage: http://www.elsevier.com/locate/ejmech

Short communication

Optimization of a fragment linking hit toward Dengue and Zika virus NS5 methyltransferases inhibitors

Jessica Hernandez [a], Laurent Hoffer [a], Bruno Coutard [b], Gilles Querat [c], Philippe Roche [a], Xavier Morelli [a], Etienne Decroly [b], Karine Barral [a, *]

[a] Aix-Marseille Univ, CNRS UMR7258, INSERM U1068, Institut Paoli-Calmettes, CRCM, Marseille, France
[b] Aix-Marseille Univ, CNRS, AFMB UMR 7257, Marseille, France
[c] UMR190, Emergence des Pathologies Virales, Aix-Marseille Univ, IRD French Institute of Research for Development, EHESP French School of Public Health, 27 Boulevard Jean Moulin, Marseille, 13005, France

ARTICLE INFO

Article history:
Received 30 May 2018
Received in revised form
15 September 2018
Accepted 23 September 2018
Available online 23 October 2018

Keywords:
Fragment growing
Structure-based drug design
Dengue and Zika viruses
Flavivirus NS5 methyltransferase inhibitors

ABSTRACT

No antiviral drugs to treat or prevent life-threatening flavivirus infections such as those caused by mosquito-borne Dengue (DENV) and more recently Zika (ZIKV) viruses are yet available. We aim to develop, through a structure-based drug design approach, novel inhibitors targeting the NS5 AdoMet-dependent mRNA methyltransferase (MTase), a viral protein involved in the RNA capping process essential for flaviviruses replication. Herein, we describe the optimization of a hit (**5**) identified using fragment-based and structure-guided linking techniques, which binds to a proximal site of the AdoMet binding pocket. X-ray crystallographic structures and computational docking were used to guide our optimization process and lead to compounds **30** and **33** (DENV $IC_{50} = 26\,\mu M$ and $23\,\mu M$; ZIKV $IC_{50} = 28\,\mu M$ and $19\,\mu M$, respectively), two representatives of novel non-nucleoside inhibitors of flavivirus MTases.

1. Introduction

Mosquito-borne flaviviruses, such as Dengue (DENV), West Nile (WNV), Zika (ZIKV), Japanese encephalitis (JEV) and Yellow fever (YFV) viruses provide the most frequent cause of emerging and resurging life-threatening diseases of global significance. In particular, DENV and ZIKV have become major international public health concerns. Indeed, the four serotypes of dengue virus affecting human (DENV1-4) are the most prevalent mosquito-borne viral disease of humans and cause around 300 million human infections annually, leading to about 30,000 deaths/year upon hemorrhagic dengue fever. Their transmission has increased dramatically in urban and semi-urban areas, because of global climate changes and international traveling. In addition, a recent widespread epidemic of ZIKV disseminated to South and to North America, with 2 million suspected infected cases. ZIKV is causative agent of neurological disorders such as microcephaly in newborns or Guillain-Barre syndrome in adults [1–3]. To date, there are no approved antiviral compounds to treat DENV or ZIKV infections. In such a context, the development of potent antiviral compounds to prevent or treat these infections is crucial. A natural target is the flaviviral replication machinery and more particularly enzymes whose inhibition could block viral replication and/or increase antiviral immune response.

Flavivirus are positive single-stranded RNA viruses carrying a cap-1 structure ($^{7Me}GpppA_{2'OMe}$-RNA) at the 5′-end of their genome [4,5]. The replication of the genome is ensured by the viral replication/transcription complex, composed of five nonstructural (NS) proteins [6]. The flaviviral methyltransferase (MTase) is located at the N-terminus of NS5 and catalyzes two methylation reactions involved in the synthesis of the cap structure: methylation of the cap guanine at its N7-position to yield $^{7Me}GpppA$-RNA and methylation of the first transcribed nucleotide at its 2′-O-position to yield $^{7Me}GpppA_{2'OMe}$-RNA [7–9]. These modifications are essential for the formation of the mature RNA cap-1 structure and required for the replication of Flaviviruses [10–13] as they protect viral mRNAs from cellular 5′-exonucleases, allow the recruitment of the cellular eIF4e factor for translation initiation, and hide viral RNAs from detection by innate immunity sensors such as RIG-I, MDA5 and interferon induced restriction factors such as IFIT

* Corresponding author.
E-mail address: karine.barral@inserm.fr (K. Barral).

https://doi.org/10.1016/j.ejmech.2018.09.056
0223-5234/

Abbreviations

DENV	dengue virus
WNV	West Nile virus
ZIKV	Zika virus
NS	non-structural protein
MTase	methyltransferase
AdoMet	*S*-Adenosyl-L-methionine
AdoHcy	*S*-Adenosyl-L-homocysteine
FBDD	fragment-based drug discovery
FBS	fragment-based screening
FBS-X	FBS by X-ray crystallography
HTS	High throughput screening
PDB	protein data bank
BB	building block
TSA	thermal-shift assay
MS	mass spectrometry
NMR	nuclear magnetic resonance
IC_{50}	inhibitory concentration causing 50% reduction in enzyme activity
EC_{50}	effective concentration inducing 50% of the maximum effect on infected cells
CC_{50}	cytotoxic concentration that reduces the infected cell number by 50%
SD	standard deviation
LC/MS	liquid chromatography/mass spectroscopy
MW	molecular weight
rt	room temperature
MAOS	Microwave-assisted organic synthesis
DIPEA	*N*,*N*-Diisopropylethylamine
TEA	Triethylamine
DMAP	*N*-(3-dimethylaminopropyl)-*N*′-ethylcarbodiimide hydrochloride
AcOEt	Ethyl acetate
THF	tetrahydrofuran
DMF	dimethylformamide
FA	formic acid
VS	virtual screening

molecules [5]. Thus, both N7- and 2′*O*-MTase activities are relevant targets for drug design.

Flaviviral MTases use *S*-Adenosyl-L-methionine (AdoMet) as the methylating cofactor. Since host cells express a range of AdoMet-dependent MTases essential for cellular functions, it is essential to identify highly selective molecules for the development of viral MTase inhibitors. To date, compounds described to affect DENV or ZIKV MTase activities are AdoMet analogues or compounds identified by HTS or *in silico* screening targeting the AdoMet binding site [14–17] which is conserved in most of cellular MTases. In such a context, the identification of suitable new target sites for the development of new anti-Flavivirus remains a major challenge [18]. For this purpose, we recently reported seven fragments hits that bind DENV MTase [19] identified by a primary fragment-based screening using a thermal-shift assay (TSA) followed by a fragment-based X-ray crystallographic screening (FBS-X). Three of these fragment hits, namely **1**–**3** (Fig. 1A), individually bind outside but still close to AdoMet binding pocket, highlighting the opportunity to develop inhibitors targeting new allosteric sites (see PDB codes 5EKX for **1**, 5EIW for **2** and 5EIF for **3**) [19]. Based on X-ray crystallographic complex structures between DENV MTase and fragments **1** to **3**, we performed a 'fragment-linking' strategy consisting in the chemical linking of these fragments to give higher affinity-binding compounds. Computational modeling methods were used to design linkers with optimal length, rigidity and suitable chemical properties. Analogues containing these chemical linkers were synthesized and two urea linker derivatives, **4** and **5**, were observed in complex with crystal structures of DENV MTase (Fig. 1B and C, **4** PDB code 5EC8 and **5** PDB code 5E9Q) [20]. Then, we selected urea derivatives **4** and **5**, whose binding mode is known, for a second round of optimization, and generated analogues by adding chemical groups that might bind to additional parts of DENV MTase. A new ring with a carboxylate moiety in the *para*-position was linked to the original scaffold (ureas **4** and **5**) with a sulphonic ester or sulphonamide linker (See examples in Fig. 1D and E) [20].

Thus, a novel series of non-nucleoside inhibitors of flavivirus MTase (**6**–**11**) was synthesized displaying a 10–100-fold stronger inhibition of DENV, WNV and ZIKV 2′-*O*-MTase activities compared to original fragments with IC_{50} values from 91 μM to 452 μM, 51 μM–299 μM and 24 μM–221 μM respectively (see Table S1 in supplementary data) [20,21]. These results demonstrated the feasibility of a FBDD approach on DENV NS5 and highlighted a new suitable site for the development of new classes of inhibitors targeting flaviviral cap MTases. However, the inhibition potency of these compounds (**6**–**11**) on MTase activities did not reach the low micromolar range which is consistent with the crystallographic data. Indeed, electron-density maps for compounds **6** and **7** (Fig. 1D and E, PDB code 5EHI for **6** and PDB code 5EHG for **7**) showed a partial occupancy for the third phenyl ring, suggesting that it contributes poorly to the binding with DENV MTase. Based on these results, we performed a novel fragment-growing optimization process starting from urea derivatives **4** and **5**, to generate new analogues by adding chemical groups that might establish strong interactions with flaviviral MTases.

2. Results and discussion

2.1. Growing-based optimization of urea derivative compounds

Based on X-ray crystallographic structure of DENV MTase in complex with compound **5**, a molecular modeling strategy was applied to the design of new set of ZIKV MTase inhibitors. Indeed, both inhibitors **8** and **11**, which share the core structure of **5**, were reported as inhibitors of ZIKV MTase using an experimental assay. The hypothesis of the conserved binding mode was also based on the very high structural identity between MTase from both viruses [21]. Finally, the analysis of X-ray structures revealed a nearby cluster of arginine residues (R37, R41, R57 and R84) that could be targeted.

The *in silico* pipeline can be briefly described as follows (see M&M for details): a focused virtual chemical library was first designed using compound **5** core substructure, encoded organic chemistry rules [22] and commercially available building blocks. All the generated compounds contained a shared substructure, making it a focused library. This chemistry-driven strategy created molecules with good synthetic accessibility. This raw focused library was huge and contained duplicates or very similar compounds, so it was post-processed mainly to 1) discard those with either undesirable moieties to medicinal chemists or unreasonable physiochemical properties, and 2) extract a representative subset of compounds having high diversity. Then, this final subset was virtually screened

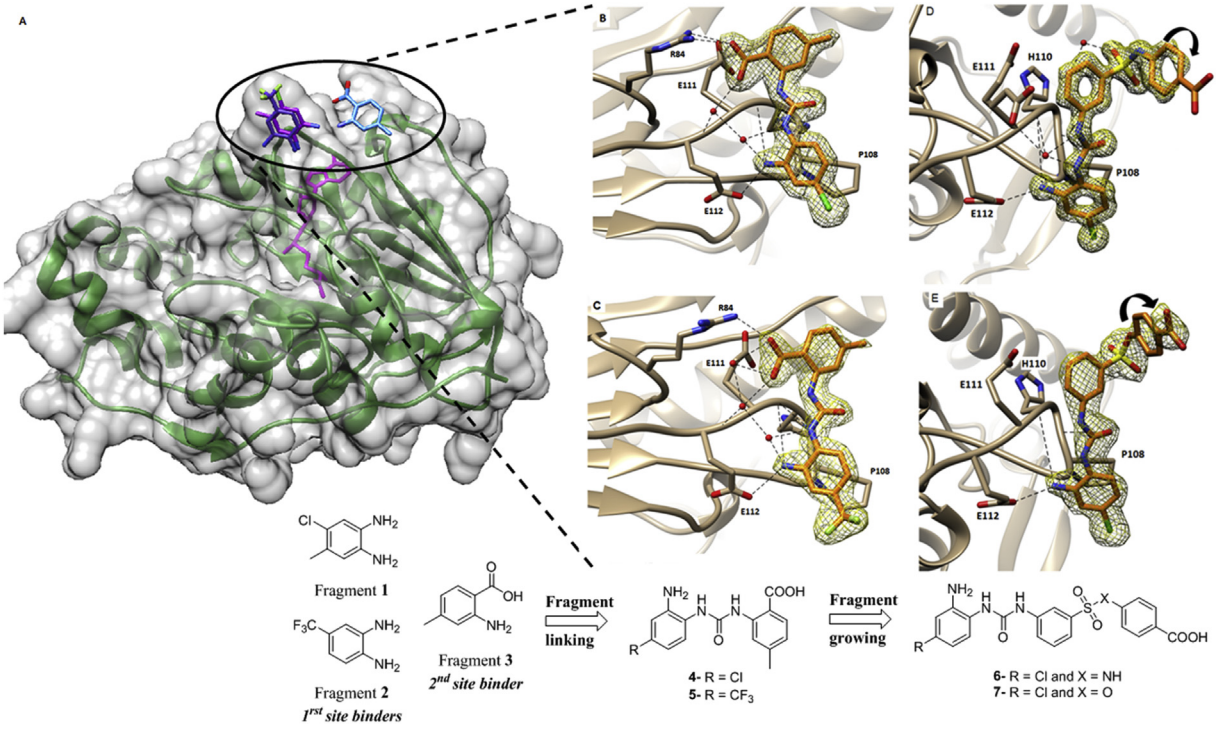

Fig. 1. (**A**) Chemical structures of fragment hits **1**–**3** and view of the DENV3 MTase crystal structure (backbone in green with molecular surface in gray) and AdoMet (shown in magenta) in complex with fragments **1** (in purple), **2** (in medium blue) and **3** (in cyan). (**B**) Crystal structure of DENV-3 MTase in complex with bound urea derivative **4**. (**C**) Crystal structure of DENV-3 MTase in complex with bound urea derivative **5**. (D) Crystal structure of DENV-3 MTase in complex with bound compound **6**. (E) Crystal structure of DENV-3 MTase in complex with bound compound **7.** Urea derivatives **4**–**5** and compounds **6**–**7** are shown in cylinder representation orange carbon atom. Nitrogen, oxygen, sulfur, chlorine and fluorine are colored in blue, red, yellow, green and light green, respectively. Small red spheres represent water molecules around the binding sites. Hydrogen bond interactions are shown as black dotted lines. Amino acid residues shown are those establishing Van der Waals interactions with the urea derivative. In the insets, F_o-F_c omits electron density maps are shown as a yellow mesh contoured at 1.6σ around the urea derivative. (For interpretation of the references to color in this figure legend, the reader is referred to the Web version of this article.)

using the S4MPLE molecular modeling tool [23,24] with constraints on the shared substructure according to the generic growing paradigm in fragment-based drug discovery.

The prioritization of the compounds was based on several criteria, the most important one being the interaction energy. In practice, the best poses within an energy window of 1 kcal/mol from the top 3% ranked compounds were considered for further analysis. However, putative optimizations involving a significant shift in the binding mode of the reference substructure after the constraint-free energy minimization were discarded because the original interactions were lost. This shift was automatically measured using the RMSD criterion between the original and final locations of flagged reference atoms. It should be noted that significant RMSD shifts were measured for numerous compounds evaluated in this project, highlighting that the reference substructure is moderately anchored to the protein. As a consequence, a cut-off value of 1.25 Å was used to discard poses with too large shift. The remaining poses were subjected to visual inspection with the Pymol tool (http://pymol.org). Of note, previously described compounds **8** and **11** were automatically built during the creation of the virtual focused library. Despites their moderate affinity, they were both ranked in the top hit-list (top 0.4%). In the end, twelve compounds that converged towards the targeted arginine clusters were selected, all but one containing a negatively charged carboxylate group (Table 1).

Then, we focused on the synthesis of these new urea linker derivatives reported in Table 1. A general synthesis of the sulfonamide derivatives is depicted in Scheme 1. To proceed, we condensed the commercial 2-nitro-4-(trifluoromethyl)phenyl isocyanate **12** (Scheme 1) with 2-aminobenzenesulfonic acid **13** and 3-aminobenzenesulfonic acid **14** under basic conditions. Two different experimental methods (a and b) were applied and compared, the first one under conventional heating at 80 °C in DMF during 6–8 h [20,25,26], and the second one with MAOS at 120 °C in acetonitrile during 5min [27,28]. Both methods provided the desired ureas **15**–**16** with excellent yields. Phosphorous oxychloride was used to convert sulfonic acid derivatives **15**–**16** to their corresponding sulfonyl chloride intermediates that were directly coupled with the appropriate amine derivatives in a mixture pyridine/THF at room temperature to give sulfonamide derivatives **17**–**22** with moderate to low yields.

After several attempts using described procedures, we were not able to react the sulfonyl chloride intermediate **16** with the commercial (2-aminomethyl)phenylacetic acid corresponding to the selected compound VS06 described in Table 1, probably because of the steric hindrance due to its *ortho*-substitution.

The aryl nitro group of **17**–**22** was reduced to aniline with stannous chloride in ethyl acetate at 60 °C yielded the desired derivatives **23**–**25**, **27**–**28** [29–32]. Compound **20** was reduced in a similar way, then hydrolyzed with LiOH to give the desired carboxylic acid derivative **26** with a final yield of 60% (Scheme 1). The reduction of aryl nitro group (**17**–**22**) was attempted with catalytic hydrogenation using Pd/C and with Clemmensen conditions (Zn/HCl) in EtOH but these reaction conditions gave very low yields.

We also focused on the synthesis of sulfone ester derivatives (Scheme 2). As previously, we used phosphorous oxychloride to convert sulfonic acid derivative **16** to its corresponding sulfonyl chloride derivative **29**, which was then coupled with commercial 3-

Table 1
2D structure of selected compounds by the virtual growing strategy. Building blocks used to build the compounds are shown with reactive groups leading to sulfonamide or sulfone ester functions highlighted in red. Rank and growing in para or meta position are mentioned for each compound. Both reference inhibitors **8** and **11** are displayed with a grey background.

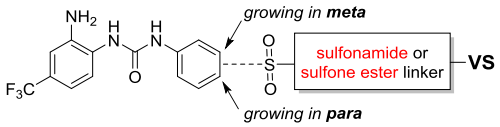

VS ID	Substructure&growing position	Top% from VS	VS ID	Substructure&growing position	Top% from VS
VS01	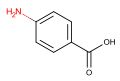 growing in **para**	0.2	**VS07**	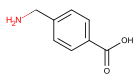 growing in **meta**	0.7
	growing in ***para***			*growing in* ***meta***	
VS02	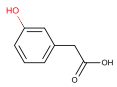 growing in **para**	0.3	**VS08**	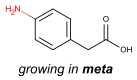 growing in **meta**	1.0
	growing in ***para***			*growing in* ***meta***	
VS03	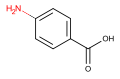 growing in **meta**	0.4	**VS09**	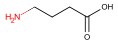 growing in **meta**	1.5
	growing in ***meta***			*growing in* ***meta***	
VS04	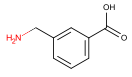 growing in **meta**	0.5	**VS10**	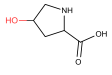 growing in **meta**	2.6
	growing in ***meta***			*growing in* ***meta***	
VS05	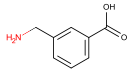 growing in **para**	0.6	**VS11**	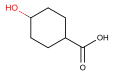 growing in **meta**	2.8
	growing in ***para***			*growing in* ***meta***	
VS06	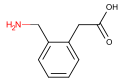 growing in **para**	0.7	**VS12**	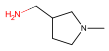 growing in **para**	2.9
	growing in ***para***			*growing in* ***para***	

hydroxyphenylacetic acid in the presence of trimethylamine and DMAP in dichloromethane to give the desired sulfone ester derivative **30** (38%) and, surprisingly, the sulfone ester derivative **31** (16%). The formation of compound **31** is probably due to traces of $POCl_3$ activating the carboxylic acid of derivative **30** to its acyl chloride intermediate that reacts with 3-hydroxyphenylacetic acid added in excess.

The previously used reaction conditions to obtain the sulfonamide derivatives **17**–**22** (Scheme 1), i.e. a mixture pyridine/THF, did not lead to the synthesis of compound **30** and were replaced by the use of triethylamine and DMAP in dichloromethane at room temperature [33,34]. In the same manner, we attempted unsuccessfully to react the sulfonyl chloride intermediate **15** with the commercial *trans*-4-hydroxy-L-proline and *trans*-4-hydroxycyclohexanecarboxylic acid corresponding to the selected compounds VS10 and VS11, respectively (see Table 1). Despite several attempts in different reaction conditions, we were not able to synthesize these two sulfone ester derivatives, probably because of the low reactivity of their secondary alcohol functional group.

The aryl nitro group of sulfone ester derivatives **30** and **31** was reduced to aniline with stannous chloride in ethyl acetate at 60 °C yielded the desired derivative **32** and the unexpected derivative **33**, respectively.

2.2. Determination of IC_{50} on DENV and ZIKV 2′O-MTase activities and antiviral evaluation on DENV and ZIKV infected cells

The newly synthetized derivatives **17**–**28** and **30**–**33**, including the aryl nitro intermediates from the next-to-last step, were then evaluated for inhibitory activity in DENV-3 as well as in ZIKV 2′-*O*-MTase assays, by measuring the inhibition of [^{3}H]-AdoMet transfer onto short synthetic capped RNA ($GpppAC_4$) [21,35].

As shown in Table 2, compounds **20**, **22**, **26** and **28** that do not contain a third phenyl ring linked to the original scaffold (ureas **4** and **5**) with a sulphonic ester or sulphonamide linker display none (or low) inhibition on DENV-3 and ZIKV 2′-*O*-MTase activities. Compounds **17**–**18** and **23**–**25** containing a third phenyl ring linked to the original urea scaffold in *meta* position with a sulfonamide

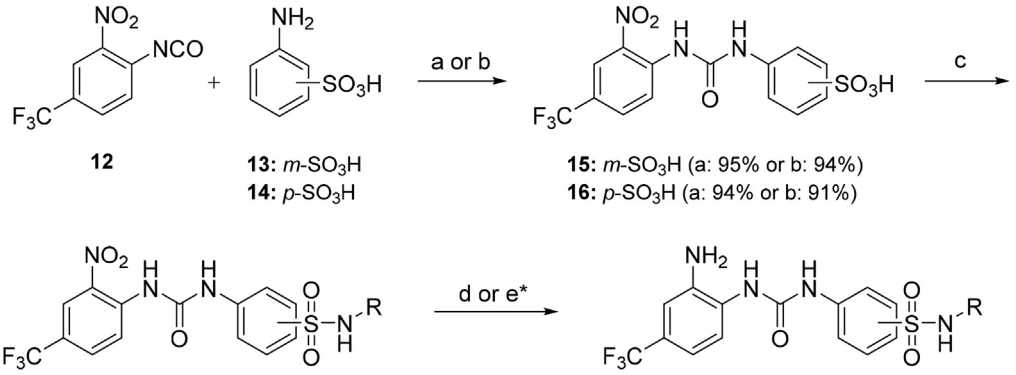

17: *m*-SO_2NHR; R = 4-phenylacetic acid (44%)
18: *m*-SO_2NHR; R = methyl-3-benzoic acid (30%)
19: *m*-SO_2NHR; R = methyl-4-benzoic acid (10%)
20: *m*-SO_2NHR; R = methyl butanoate (9%)
21: *p*-SO_2NHR; R = methyl-3-benzoic acid (12%)
22: *p*-SO_2NHR; R = methyl-*N*-(1-methylpyrrolidin-3-yl) (31%)
23 (VS06)**:** *m*-SO_2NHR; R = 4-phenylacetic acid (15%)
24 (VS04)**:** *m*-SO_2NHR; R = methyl-3-benzoic acid (16%)
25 (VS07)**:** *m*-SO_2NHR; R = methyl-4-benzoic acid (78%)
26* (VS09)**:** *m*-SO_2NHR; R = butanoic acid (60%)
27 (VS05)**:** *p*-SO_2NHR; R = methyl-3-benzoic acid (35%)
28 (VS12)**:** *p*-SO_2NHR; R = methyl-*N*-(1-methylpyrrolidin-3-yl) (27%)

Reagents and conditions: (a) DIPEA, dry DMF, 80°C, 6-8h or (b) DIPEA, dry CH_3CN, 120°C, MW, 5min; (c) $POCl_3$, 0°C to rt-60°C, 2-4h, then NH_2R, dry pyridine, dry THF, rt-18h; (d) $SnCl_2$, AcOEt, 60°C, 2-8h; (e*) $SnCl_2$, AcOEt, 60°C, 3h, then LiOH, THF/H2O, 0 °C to rt, 2h (only to obtain compound **26**).

Scheme 1. Synthesis of sulfonamide derivatives **17**–**28.**

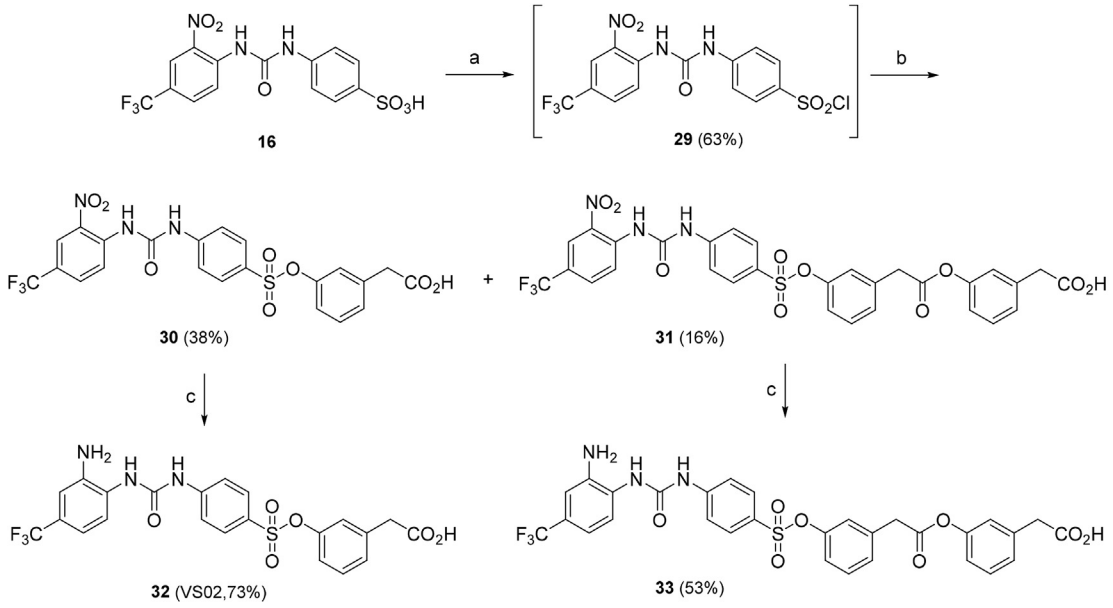

Reagents and conditions: (a) $POCl_3$, 0°C to rt-60°C, 3h; (b) 3-hydroxyphenylacetic acid, dry CH_2Cl_2, TEA, DMAP, rt, 18h; (c) $SnCl_2$, AcOEt, reflux, 2-8h.

Scheme 2. Synthesis of sulfone ester derivatives **30**–**33.**

bond display low to moderate inhibition on DENV-3 and ZIKV 2′-*O*-MTase activities. Derivative **23** substituted with a 4-phenylacetic acid group display slightly higher (DENV) or comparable (ZIKV) 2′-*O*-MTase activities inhibition than derivatives **24** and **25** substituted with methyl-3-benzoic acid and mehyl-4-benzoic acid groups (IC_{50} DENV MTase of 144 μM, 304 μM and 366 μM, and IC_{50} ZIKV MTase of 135 μM, 95 μM and 122 μM, respectively).

Derivatives containing a third phenyl ring linked to the original urea scaffold in *para* position with a sulphonamide or sulphonic ester linker resulted in more potent compounds. Indeed, by comparison with derivatives **18** and **24**, their sulfonamide analogues **21** and **27** substituted in *para* position with the same methyl-3-benzoic acid group showed higher inhibition effects with IC_{50} DENV of 145 μM and 174 μM, and IC_{50} ZIKV of 83 μM and 61 μM,

Table 2
IC_{50} determination of compounds **17**–**28** and **30**–**33** on DENV-3 and ZIKV 2′-*O*-MTase assays.

Entry	Structure	DENV 2′*O*-MTase activity IC_{50} (μM)[a]	ZKV 2′*O*-MTase activity IC_{50} (μM)[a]	Entry (VS ID)	Structure	DENV 2′*O*-MTase activity IC_{50} (μM)[a]	ZKV 2′*O*-MTase activity IC_{50} (μM)[a]
17	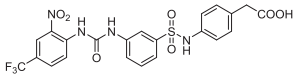	181 ± 12	185 ± 12	**23** (VS08)	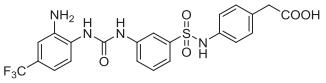	144 ± 8	135 ± 11
18	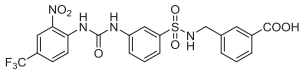	> 400	136 ± 12	**24** (VS04)	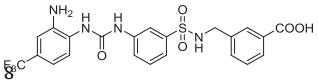	304 ± 29	95 ± 12
19	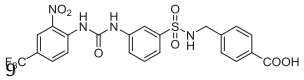	nd	nd	**25** (VS07)	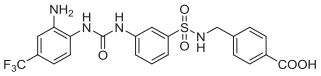	366 ± 16	122 ± 15
20	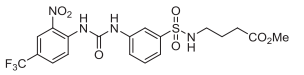	> 400	> 400	**26** (VS09)	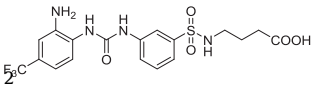	342 ± 33	132 ± 23
21	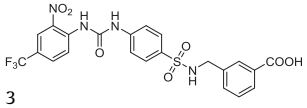	145 ± 5	83 ± 8	**27** (VS05)	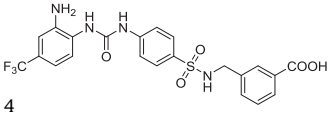	174 ± 10	61 ± 6
22	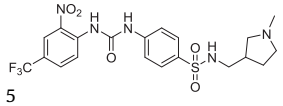	> 400	> 400	**28** (VS12)	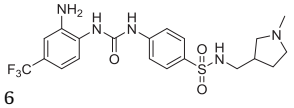	> 400	> 400
30	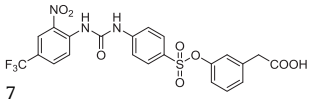	26 ± 2	28 ± 3	**32** (VS02)	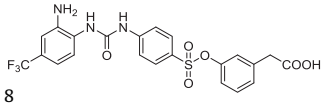	276 ± 15	111 ± 12
31	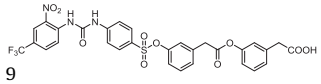	nd	nd	**33**	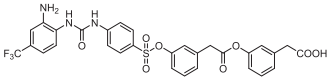	24 ± 2	19 ± 2

respectively. Interestingly, aryl nitro intermediates **17**, **18** and **21** exhibit slightly comparable inhibition potential than their aniline analogues **23**, **24** and **27**, respectively. However, derivatives **30**, **32** and unexpected **33** linked to the original urea scaffold in *para* position with a sulphonic ester linker and substituted with a 3-phenylacetic acid group are those that display the best inhibitory effect with IC_{50} DENV values of 26 μM, 276 μM and 24 μM, and IC_{50} ZIKV values of 28 μM, 111 μM and 19 μM, respectively. Surprisingly, in this unique case, the aryl nitro intermediate **30** exhibits a more potent inhibition effect than its aniline analogue **32**. Unfortunately, the inhibitory activity of unexpected aryl nitro intermediate **31** (from the double coupling reaction with 3-hydroxyphenylacetic acid) could not be evaluated since the small amount obtained was fully used for the synthesis of compound **33**.

The most efficient inhibitors **21**, **27**, **30** and **33** identified on DENV and ZIKV MTases ($IC_{50} \leq 100$ μM) were evaluated for their potential inhibitory effect on the *in vitro* replication of DENV and ZIKV in Vero E6 cells. The inhibition was determined by quantifying the virus replication using a RT-PCR assay as previously described [36]. None of the compounds showed any potent inhibition on DENV-2 (Toulon strain, CNR 25,679 EVAg ref 001V-02229) or ZIKV (French Polynesia strain, H/PF/2013 EVAg ref 001 V-EVA1545) up to 20 μM. No cytotoxicity was observed up to 100 μM for compounds **27** and **33**. However compounds **21** and **30** displayed CC_{50} values of 70 μM and 37.5 μM, respectively. The observed cytotoxic effect exhibited by compounds **21** and **30** might be due to the presence of aromatic nitro groups that are well-known toxicophores [37] and demonstrate a low cell membrane permeation. The lack of any activities in the virus inhibition assay and the cell cytotoxicity assay for compounds **27** and **33** could be due either to an intrinsic low activity of the compounds *ex vivo* or to poor abilities to cross cell membranes.

3. Conclusion

To improve the potency of a fragment linking hit (urea **5**), identified during a previous FBDD campaign as an attractive starting point for inhibitory design that bound to a proximal pocket of DENV MTase, we developed a rapid pathway based on X-ray crystallographic structures and computational docking to guide the fragment growing process. Efforts focused on optimization of interactions in and close to the binding pocket allowed the synthesis of new derivatives that inhibit two important flavivirus 2′-*O*-MTase activity, DENV and ZIKV respectively, in the micromolar range. Only derivatives containing a third phenyl ring linked to the original urea scaffold display DENV and ZIKV 2′-*O*-MTase activities inhibition. Derivatives containing a third phenyl ring substituted in *para* (versus *meta*) position and with a sulphonic ester (versus sulphonamide) linker display a higher inhibition potential. Interestingly, for these last compounds, aryl nitro intermediates exhibit comparable (**21**) or even higher (**30**) inhibition effect than their aniline analogues (**27** and **32**, respectively). Furthermore, unexpected derivative **33**, linked to the original urea scaffold in *para* position with a sulphonic ester linker and substituted with a 3-phenylacetic acid group, surprisingly display the best inhibitory effect. Thereby, the most potent inhibitors **30** and **33** showed an efficient inhibition of

MTase activity with IC_{50} values ~20 μM (DENV $IC_{50} = 26$ μM and 24 μM; ZIKV $IC_{50} = 28$ μM and 19 μM, respectively). Although the inhibition potency of our compounds on MTase activities did not reach the low micromolar range, these results validate a suitable allosteric site for the development of new classes of inhibitors targeting flaviviral cap MTases.

4. Experimental section

4.1. Molecular modeling

4.1.1. Binding site preparation

The X-ray structure of the NS5 methyltransferase from Zika virus bound to S-adenosylmethionine (PDB code 5KQR [38]) was beforehand superposed to the X-ray structure of its Dengue virus homologue (PDB code 5E9Q [20]) which contains the reference inhibitor. Then, the Zika 5KQR structure was prepared using MOE version 2016 (Chemical Computing Group Inc., Montreal, QC, Canada) to explicitly add hydrogens and define the binding site. A probe atom was placed inside the arginine cluster. All residues, with at least one atom within 12 Å radius from either reference substructure ("3-[2-amino-4-(trifluoromethyl)phenyl]-1-phenylurea") or probe atom, were selected to define the binding site. A large binding site was defined because S4MPLE relies on a force field-based energy function.

4.1.2. Library design

The choice of considered chemical reactions was based on already synthesized intermediates: **15** (meta) and **16** (para). Two reactions were selected: sulfonamidation and sulfo-esterification. Both of them require a sulfonyl-chloride group as reactant (Fig. 1). An in house python script, based on the RDKit toolkit (http://www.rdkit.org), was used to create the raw focused library in the SMILES format starting from 1) the intermediates **15** and **16**, 2) the two selected chemistry rules, and 3) a pre-processed database of commercially available BBs.

Several post-processing stages were applied to this huge raw virtual library that initially contained 61,338 molecules. First, a structural check was performed with StructureChecker from ChemAxon (http://www.chemaxon.com) to eliminate compounds with any structural warning. Duplicates and compounds that contain at least one undesired element (other than C, H, N, O, P, S, F, Cl, Br or I) were also discarded. Usual threshold values for common physico-chemical descriptors (molecular weight ≤ 550, cLogP ≤ 5.5, tPSA ≤ 150 Å^2, rotational bond count ≤ 12, and ring system size ≤ 2) were used to automatically extract a subset of compounds with reasonable properties. Then, yuck filters, which were used to design the clean subset of the ZINC database (http://zinc.docking.org), were employed to reject compounds with undesired functional groups. Cxcalc and Jcsearch programs from ChemAxon were respectively used to compute descriptors and detect undesired substructures.

A clustering strategy was then performed to extract a representative subset of diverse compounds. In practice, molecules were simplified with deletion of halogen and pruning of terminal acyclic hydrophobic moieties. Clusters were generated by identifying identical structures. The representative subset of diverse compounds was simply created by picking the less decorated entity (for instance, the original compound with the lowest molecular weight) from each cluster. This clustering strategy, which appears as a less stringent version of the Bemis-Murcko-based approach [39], greatly decreases the number of compounds to consider. However, different stereoisomers and some slight variations in heterocycles or polar groups, that may be crucial in the first cycle of hit-to-lead optimization, were still present in the database.

The last processing stage involved various computations which were required for the subsequent VS. Major microspecies, partial charges, force-field atomic types, and a single 3D-conformer were computed for each compound. The reference substructure, constrained during the VS, was defined as the "3-(trifluoromethyl) aniline" moiety, and corresponding atoms from each designed molecule were flagged using a maximum common substructure (MCS) algorithm. Finally, the generated conformers were automatically superimposed to the pre-positioned reference structure within the binding site. Mapping of force-field atomic types was done using programs from AmberTools (http://ambermd.org), while all the other steps were performed using in house tools relying on the ChemAxon Java API. The final virtual focused chemical library contained 5712 molecules.

4.1.3. Virtual screening

The final subset of 5712 compounds was virtually screened using S4MPLE with constraints on the original location of the "3-(trifluromethyl)aniline" substructure. Other moieties, including the newly added atoms from virtual synthesis, were free to explore adjacent subpockets without any constraints. The conformational sampling search was performed as previously described [23], and mainly consisted in 3 independent simulations of 400 generations with a population of 30 individuals. The post-processing stage consisted in the energy minimization of all non-redundant poses, after all constraints were previously removed. Another simulation with the sole ligand was also performed in order to find its lowest energy conformer. The ranking criterion was defined as the difference between lowest potential energy of the complex and the lowest potential energy of the ligand alone.

4.2. Chemistry

All reagents and solvents were purchased from Sigma Aldrich or Acros Organics companies. Analytical thin layer chromatographies (TLC) were performed on silica gel 60F 254 aluminium plates (Merck) of 0.2 mm thickness with appropriate solvents. The spots were examined with UV light ($\lambda = 254$ nm) and Ninhydrin Spray. Preparative flash column chromatographies were performed using silica gel (Merck) G60 230–240 under compressed air. The ^{1}H NMR and ^{13}C NMR spectra were determined with a BRUCKER AMX 250 MHz or BRUKER Avance III nanobay 400 MHz. Chemical shifts are expressed in ppm and coupling constants (*J*) are in hertz (s = singlet, bs = broad singlet, d = doublet, bd = broad doublet, dd = double doublet, ddd = double double doublet, t = triplet, bt = broad triplet, dt = double triplet, p = pentuplet or quintuplet, m = multiplet). Reaction monitoring and purity of compounds were recorded by using analytical Agilent Infinity high performance liquid chromatography (Column Zorbax SB-C18 1.8 μM (2.1 × 50 mm); Mobile phase (A: 0.1% FA H_2O, B: 0.1% FA CH_3CN, Time/%B: 0/10, 4/90, 7/90, 9/10, 10/10); Flow rate 0.3 mL/min; Diluent MeOH) with DAD at 230 nM. All tested compounds yielded data consistent with a purity of ≥95%. Low-resolution mass spectra were obtained with Agilent SQ G6120B mass spectrometer in positive and/or negative electrospray modes. Resolution Mass Spectra (HRMS) were obtained on a SYNAPT G2-S WATERS mass spectrometer.

4.2.1. General procedure for synthesis of urea derivatives ***15–16*** *by conventional heating (method A) or by MAOS (method B)*

4.2.1.1. Method A. To a stirred solution of aminobenzenesulfonic acid (1eq, 4.3 mmol) in anhydrous dimethylformamide at 0 °C under argon atmosphere was added diisopropylethylamine (3 eq, 12.9 mmol). Then, a solution of 2-nitro-4 (trifluoromethyl)phenyl isocyanate (1 eq, 4.3 mmol) in DMF was added dropwise at 0 °C.

The mixture was heated and stirred at 80 °C during at least 7 h. The solvent was removed *in vacuo*. Obtained crude residue was diluted in ethyl acetate and washed once with water, once with brine, dried over Na_2SO_4, and evaporated *in vacuo* to afford a crude residue which was purified by flash column chromatography eluting with dichloromethane-methanol (90:10 to 85:15) to give the corresponding urea derivative **15** or **16**.

4.2.1.2. Method B. Into a microwave vial charged with a stirred solution of aminobenzenesulfonic acid (2 eq, 2.0 mmol) in anhydrous acetonitrile under argon atmosphere, diisopropylethylamine was added (2.5 eq, 2.5 mmol). Then, a solution of 2-nitro-4 (trifluoromethyl)phenyl isocyanate (1 eq, 1.0 mmol) in acetonitrile was added dropwise. Vial was sealed and the mixture was irradiated, heated at 120 °C and stirred during 5 min. After completion, the solvent was removed *in vacuo* and residue was diluted in ethyl acetate, washed once with 1 N HCl, once with water, once with brine, dried over Na_2SO_4, and concentrated *in vacuo* to afford a crude residue which was purified by flash column chromatography eluting with dichloromethane-methanol (90:10 to 85:15).

*4.2.1.3. 3-({[2-nitro-4-(trifluoromethyl)phenyl]carbamoyl}amino) benzene-1-sulfonic acid **15**.* ^{1}H NMR (DMSO-d_6, 250 MHz): δ = 10.18 (bs, 1H), 9.93 (bs, 1H), 8.65 (d, J = 9.0 Hz, 1H), 8.40 (d, J = 1.4 Hz, 1H), 8.07 (dd, J = 9.1 Hz and J = 2.0 Hz, 1H), 7.78 (s, 1H), 7.64–7.46 (m, 1H), 7.29 (s, 1H), 7.28 (s, 1H); ^{13}C NMR (DMSO-d_6, 101 MHz): δ = 151.30, 148.96, 138.49, 138.25, 136.54, 131.12 (q, $^3J_{CF}$ = 3.1 Hz), 128.22, 123.27 (q, $^1J_{CF}$ = 271,15 Hz), 122.95 (q, $^3J_{CF}$ = 4.1 Hz), 122.81, 121.56 (q, $^2J_{CF}$ = 33.7 Hz), 120.06, 118.52, 116.14.; LC/MS (ESI): 404.1 $[M-H]^-$ and 405.9 $[M-H]^+$; yellow powder. Yield = 95% (method A) or 94% (method B).

*4.2.1.4. 4-({[2-nitro-4-(trifluoromethyl)phenyl]carbamoyl}amino) benzene-1-sulfonic acid **16**.* ^{1}H NMR (DMSO-d_6, 250 MHz): δ = 10.35 (bs, 1H), 10.07 (s, 1H), 8.55 (d, J = 8.6 Hz, 1H), 8.39 (s, 1H), 8.39 (d, J = 1.5 Hz, 1H), 8.08 (dd, J = 9.1 Hz and J = 1.8 Hz, 1H), 7.80 (bs, 1H), 7.59–7.46 (m, 1H), 7.28 (s, 1H), 7.30 (s, 1H). ^{13}C NMR (DMSO-d_6, 101 MHz): δ = 151.32, 142.88, 138.89, 138.34, 136.71, 131.07 (q, $^3J_{CF}$ = 3.1 Hz), 126.34, 123.26 (q, $^1J_{CF}$ = 271.5 Hz), 123.00, 122.94 (q, $^3J_{CF}$ = 4.2 Hz), 121,67 (q, $^2J_{CF}$ = 33.6 Hz), 117.59; LC/MS (ESI): 404.2 $[M-H]^-$ and 406.1 $[M-H]^+$; yellow powder. Yield = 94% (Method A) or 91% (Method B).

*4.2.2. General procedure for synthesis of nitro-sulfonamide derivatives **17**–**22***

Into a round bottom flask within respective urea derivative **15** or **16** (1 eq, 0.62 mmol), phosphorous chloride (30 eq, 18.50 mmol) was added slowly at 0 °C under argon atmosphere. The reaction mixture was stirred at 60 °C for at least 3 h. After completion, phosphorous chloride was evaporated *in vacuo* under argon atmosphere to afford a crude residue, which was diluted in anhydrous pyridine-tetrahydrofuran mixture (1:1). To the latter, a solution of amine derivative (4 eq, 2.48 mmol) in pyridine-tetrahydrofuran mixture was added. The reaction mixture was stirred overnight under argon atmosphere at room temperature. After completion, solvent was evaporated *in vacuo* atmosphere to afford a crude residue, which was purified by flash column chromatography as indicated for each compound to give derivatives **17**–**22**.

*4.2.2.1. 2-{4-[3-({[2-nitro-4-(trifluoromethyl)phenyl]carbamoyl} amino)benzenesulfonamido]phenyl}acetic acid **17**.* Chromatography on silica gel was eluting with CH_2Cl_2-MeOH (95:5 to 90:10). ^{1}H NMR (DMSO-d_6, 250 MHz): δ = 12.27 (bs, 1H), 10.42 (s, 1H), 10.34 (bs, 1H), 9.94 (s, 1H), 8.58 (d, J = 8.9 Hz, 1H), 8.39 (bd, J = 1.5 Hz, 1H), 8.13–8.08 (m, 1H), 8.06 (d, J = 2.1 Hz, 1H), 7.61 (dt, J = 8.0 Hz and 1.5 Hz, 1H), 7.49 (t, J = 7.8 Hz, 1H), 7.41 (dt, J = 7.8 Hz and 1.3 Hz, 1H), 7.12 (d, J = 8.6 Hz, 2H), 7.03 (d, J = 8.6 Hz, 2H), 3.45 (s, 2H). ^{13}C NMR (DMSO-d_6, 63 MHz): δ = 172.63, 151.36, 140.29, 139.63, 138.09, 136.82, 136.04, 131.18 (q, $^3J_{CF}$ = 3.6 Hz), 130.75, 130.12, 129.91, 123.22 (q, $^1J_{CF}$ = 271.6 Hz), 122.97, 122.39, 121.92 (q, $^2J_{CF}$ = 33.8 Hz), 120.69, 119.93, 116.31, 40.39; LC/MS (ESI): 537.0 $[M-H]^-$, 538.9 $[M+H]^+$; HRMS (TOF, ESI-) cald for $C_{22}H_{16}N_4O_7F_3S$ $[M-H]^-$ 537.0692, found 537.0698; yellow powder. Yield = 44%.

*4.2.2.2. 3-{[3-({[2-nitro-4-(trifluoromethyl)phenyl]carbamoyl} amino)benzenesulfonamido]methyl}benzoic acid **18**.* Chromatography on silica gel was eluting with CH_2Cl_2-MeOH (95:5 to 90:10). ^{1}H NMR (DMSO-d_6, 250 MHz): 12.96 (bs, 1H), 10.46 (s, 1H), 10.00 (s, 1H), 8.62 (d, J = 8.9 Hz, 1H), 8.40 (bd, J = 1.3 Hz, 1H), 8.32 (t, J = 6.3 Hz, 1H), 8.13–8.02 (m, 2H), 7.89–7.84 (m, 1H), 7.80 (dt, J = 7.3 Hz and 1.3 Hz, 1H), 7.65 (dt, J = 7.8 Hz and 1.3 Hz, 1H), 7.56–7.35 (m, 4H), 4.07 (d, J = 6.1 Hz, 2H). ^{13}C NMR (DMSO-d_6, 63 MHz): δ = 167.18, 151.38, 144.20, 141.28, 139.61, 138.19, 136.75, 131.94, 131.26 (q, $^3J_{CF}$ = 3.4 Hz), 130.81, 129.89, 128.43, 128.40, 128.07, 123.24 (q, $^1J_{CF}$ = 271.8 Hz), 123.00 (q, $^3J_{CF}$ = 3.7 Hz), 121.93, 121.88 (q, $^2J_{CF}$ = 33.8 Hz) 120.46, 116.29, 45.70; LC/MS (ESI): 537.1 $[M-H]^-$; HRMS (TOF, ESI-) cald for $C_{22}H_{16}N_4O_7F_3S$ $[M-H]^-$ 537.0692, found 537.0696; yellow powder. Yield = 30%.

*4.2.2.3. 4-{[3-({[2-nitro-4-(trifluoromethyl)phenyl]carbamoyl} amino)benzenesulfonamido]methyl}benzoic acid **19**.* Chromatography on silica gel was eluting with CH_2Cl_2-MeOH (95:5 to 90:10). ^{1}H NMR (MeOD-d^6, 250 MHz): δ = 8.75 (d, J = 8.6 Hz, 1H), 8.39 (d, J = 1.3 Hz, 1H), 7.97 (bt, J = 1.7 Hz, 1H), 7.90–7.82 (m, 2H), 7.78 (d, J = 8.4 Hz, 2H), 7.58–7.50 (m, 1H), 7.40–7.36 (m, 1H), 7.22 (t, J = 8.5 Hz, 2H), 4.09 (s, 2H). ^{13}C NMR (63 MHz, MeOD) δ 176.91, 153.17, 149.98, 145.59, 143.94, 142.89, 141.02, 137.29, 132.44 (q, $^3J_{CF}$ = 3.4 Hz), 131.00, 130.83, 130.77, 128.87, 128.30, 126.14, 124.54 (q, $^2J_{CF}$ = 33.8 Hz), 124.30 (q, $^3J_{CF}$ = 3.7 Hz), 124.00 (q, $^1J_{CF}$ = 269.5 Hz), 123.89, 123.65, 122.33, 118.43, 47.59. LC/MS (ESI): 538.9 $[M+H]^+$; yellow solid. Yield = 10%.

*4.2.2.4. methyl 4-[3-({[2-nitro-4-(trifluoromethyl)phenyl]carbamoyl} amino)benzenesulfonamido]butanoate **20**.* Chromatography on silica gel was eluting with CH_2Cl_2-MeOH (99:1 to 98:2). ^{1}H NMR (MeOD-d^6, 250 MHz): δ = 8.81 (d, J = 9.0 Hz, 1H), 8.45 (d, J = 1.4 Hz, 1H), 8.15–8.09 (m, 1H), 7.91 (dd, J = 9.3 Hz and 2.1 Hz, 1H), 7.69–7.59 (m, 1H), 7.51–7.42 (m, 2H), 3.59 (s, 3H), 2.88 (t, J = 6.8 Hz, 2H), 2.32 (t, J = 7.3 Hz, 2H), 1.71 (p, J = 7.0 Hz, 2H). ^{13}C NMR (MeOD-d^6, 101 MHz): δ = 173.83, 151.88, 141.29, 139.70, 138.70, 136.00, 130.99 (q, $^3J_{CF}$ = 3.0 Hz), 129.41, 123.25 (q, $^2J_{CF}$ = 34.8 Hz), 123.29 (q, $^1J_{CF}$ = 270.6 Hz), 122.85 (q, $^3J_{CF}$ = 4.3 Hz), 122.50, 122.44, 120.98, 117.05, 50.64, 41.90, 30.21, 24.58; LC/MS (ESI): 503.1 $[M-H]^-$, 504.9 $[M+H]^+$; HRMS (TOF, ESI-) cald for $C_{19}H_{18}N_4O_7F_3S$ $[M-H]^-$ 503.0848, found 503.0853; yellow solid. Yield = 9%.

*4.2.2.5. 3-{[4-({[2-nitro-4-(trifluoromethyl)phenyl]carbamoyl} amino)benzenesulfonamido]methyl}benzoic acid **21**.* Chromatography on silica gel was eluting with CH_2Cl_2-MeOH (95:5 to 90:10. ^{1}H NMR (MeOD-d^6, 250 MHz): δ = 8.81 (d, J = 8.9 Hz, 1H), 8.45 (d, J = 1.4 Hz, 1H), 7.91 (dd, J = 9.1 Hz and 1.9 Hz, 1H), 7.85–7.77 (m, 2H), 7.70 (d, J = 9.1 Hz, 2H), 7.62 (d, J = 9.1 Hz, 2H), 7.41 (bd, J = 7.6 Hz, 1H), 7.31 (t, J = 7.9 Hz, 1H), 4.08 (s, 2H). LC/MS (ESI): 538.9 $[M+H]^+$; HRMS (TOF, ESI-) cald for $C_{22}H_{16}N_4O_7F_3S$ $[M-H]^-$ 537.0692, found 537.0698; yellow solid. Yield = 12%.

*4.2.2.6. 1-(4-{[(1-methylpyrrolidin-3-yl)methyl]sulfamoyl}phenyl)-3-[2-nitro-4-(trifluoromethyl)phenyl]urea **22**.* Chromatography on aluminum oxide gel was eluting with CH_2Cl_2-MeOH (90:10). ^{1}H

NMR (MeOD-d^6, 250 MHz): δ = 8.78 (d, J = 9.0 Hz, 1H), 8.43 (d, J = 1.4 Hz, 1H), 7.89 (dd, J = 9.1 Hz and 2.2 Hz, 1H), 7.74 (d, J = 9.1 Hz, 2H), 7.67 (d, J = 9.2 Hz, 2H), 2.79 (d, J = 7.0 Hz, 2H), 2.74–2.63 (m, 1H), 2.61–2.47 (m, 2H), 2.40–2.22 (m, 2H), 2.32 (s, 3H), 2.03–1.80 (m, 1H), 1.59–1.35 (m, 1H). ^{13}C NMR (MeOD-d^6, 101 MHz): δ = 151.69, 142.93, 138.56, 136.09, 134.22, 130.98 (q, $^3J_{CF}$ = 3.4 Hz), 127.80, 123.36 (q, $^2J_{CF}$ = 34.4 Hz), 123.27 (q, $^1J_{CF}$ = 270.7 Hz), 122.87 (q, $^3J_{CF}$ = 3.9 Hz), 122.54, 118.44, 59.21, 55.32, 46.48, 40.72, 37.77, 28.12. LC/MS (ESI): 499.8 [M − H]$^-$, 501.8 [M+H]$^+$; HRMS (TOF, ESI-) cald for $C_{20}H_{21}N_5O_5F_3S$ [M − H]$^-$ 500.1215, found 500.1221; yellow oil. Yield = 31%.

4.2.3. General procedure for synthesis of aniline-sulfonamide derivatives **23**–**28**

To a solution of pure nitro-sulfonamide derivative **17**–**19** and **21**–**22** (1 eq) in AcOEt, Tin(II) chloride was added (6 eq). The reaction mixture was refluxed during 2–8 h. After completion, saturated solution of Na_2CO_3 was added dropwise until pH 7–8. Then, the organic layer was extracted with ethyl acetate and washed once with water, once with brine, dried over Na_2SO_4, and evaporated *in vacuo* to afford a crude residue which was purified by flash column chromatography as indicated for each compound to give derivatives **23**–**25** and **27**–**28**, respectively.

The same protocol was applied to the nitro-sulfonamide derivative **20** to afford the corresponding crude reduced residue (1eq, 0.065 mmol) which was directly solubilized in THF at 0 °C, and an aqueous solution of LiOH (4 eq, 0.26 mmol) was added dropwise. The resulting mixture was stirred 2 h at room temperature. After completion, THF was removed under vacuum. Then, 1 N HCl solution was added dropwise until pH 2–3 and the aqueous layer was extracted with ethyl acetate. The organic layer was washed once with water, once with brine, dried over Na_2SO_4, and evaporated *in vacuo* to afford a crude residue which was purified by flash column chromatography on silica gel eluting with dichloromethane-methanol (90:10) to give compound **26**.

4.2.3.1. 2-{4-[3-({[2-amino-4-(trifluoromethyl)phenyl]carbamoyl}amino)benzenesulfonamido]phenyl}acetic acid **23**.

Chromatography on silica gel was eluting with CH_2Cl_2-MeOH (85:15). ^{1}H NMR (MeOD-d^6, 250 MHz): δ = 7.93–7.82 (m, 1H), 7.64–7.52 (m, 1H), 7.47 (d, J = 8.3 Hz, 1H), 7.37–7.29 (m, 2H), 7.14–6.97 (m, 5H), 6.91 (dd, J = 8.3 Hz and 1.4 Hz, 1H), 3.47 (s, 2H). ^{13}C NMR (DMSO-d_6, 101 MHz): δ = 173.63, 153.16, 141.07, 140.62, 140.40, 136.49, 130.52, 130.13, 130.06, 128.57, 128.56, 125.16 (q, $^1J_{CF}$ = 271.5 Hz), 122.19, 122.10, 120.62, 120.06, 116.08, 116.00, 114.06 (q, $^2J_{CF}$ = 33.7 Hz), 113.23 (q, $^3J_{CF}$ = 3.7 Hz), 111.73 (q, $^3J_{CF}$ = 3.6 Hz), 41.54 LC/MS (ESI): 507.0 [M − H]$^-$, 508.9 [M+H]$^+$; HRMS (TOF, ESI-) cald for $C_{22}H_{18}N_4O_5F_3S$ [M − H]$^-$ 507.0950, found 507.0953; light orange solid. Yield = 15%.

4.2.3.2. 3-{[3-({[2-amino-4-(trifluoromethyl)phenyl]carbamoyl}amino)benzenesulfonamido]methyl}benzoic acid **24**.

Chromatography on silica gel was eluting with CH_2Cl_2-MeOH (90:10 to 85:15). ^{1}H NMR (MeOD-d^6, 250 MHz): δ = 7.98 (d, J = 1.7 Hz, 1H), 7.87–7.78 (m, 2H), 7.56 (dt, J = 7.1 Hz and 2.0 Hz, 1H), 7.50 (d, J = 8.2 Hz, 1H), 7.44–7.36 (m, 3H), 7.31 (t, J = 7.6 Hz, 1H), 7.08 (d, J = 1.8 Hz, 1H), 6.93 (dd, J = 8.3 Hz and 1.4 Hz, 1H), 4.08 (s, 2H). ^{13}C NMR (MeOD-d^6, 101 MHz) δ = 175.51, 155.44, 143.02, 142.74, 142.46, 141.59, 139.09, 133.15, 130.63, 130.17, 129.87, 129.71, 129.46, 128.66 (q, $^2J_{CF}$ = 39.2 Hz), 125.90, 125.86 (q, $^1J_{CF}$ = 270.9 Hz), 123.59, 121.74, 118.22, 115.48 (q, $^3J_{CF}$ = 3.8 Hz), 114.09 (q, $^3J_{CF}$ = 4.2 Hz), 47.65; LC/MS (ESI): 507.0 [M − H]$^-$, 508.9 [M+H]$^+$; HRMS (TOF, ESI-) cald for $C_{22}H_{18}N_4O_5F_3S$ [M − H]$^-$ 507.0950, found 507.0948; white solid. Yield = 16%.

4.2.3.3. 4-{[3-({[2-amino-4-(trifluoromethyl)phenyl]carbamoyl}amino)benzenesulfonamido]methyl}benzoic acid **25**.

Chromatography on silica gel was eluting with CH_2Cl_2-MeOH (90:10 to 85:15). ^{1}H NMR (MeOD-d^6, 250 MHz): δ = 7.94–7.91 (m, 1H), 7.79 (d, J = 8.4 Hz, 2H), 7.48 (dt, J = 7.0 Hz and 2.1 Hz, 1H), 7.43 (dd, J = 8.3 Hz and 0.5 Hz, 1H), 7.37–7.31 (m, 2H), 7.21 (d, J = 8.4 Hz, 2H), 7.01 (d, J = 1.9 Hz, 1H), 6.89 (ddd, J = 8.3 Hz, 2.0 Hz, and 0.6 Hz 1H), 4.06 (s, 2H). LC/MS (ESI): 506.9 [M − H]$^-$, 508.9 [M+H]$^+$; HRMS (TOF, ESI-) cald for $C_{22}H_{18}N_4O_5F_3S$ [M − H]$^-$ 507.0950, found 507.0957; pale yellow powder. Yield = 78%.

4.2.3.4. 4-[3-({[2-amino-4-(trifluoromethyl)phenyl]carbamoyl}amino)benzenesulfonamido]butanoic acid **26**.

Chromatography on silica gel was eluting with CH_2Cl_2-MeOH (90:10). ^{1}H NMR (MeOD-d^6, 250 MHz): δ = 8.05–7.99 (m, 1H), 7.63–7.53 (m, 1H), 7.47 (bd, J = 8.2 Hz, 1H), 7.43 (d, J = 0.8 Hz, 1H), 7.42 (d, J = 1.7 Hz, 1H), 7.05 (d, J = 1.8 Hz, 1H), 6.90 (dd, J = 8.3 Hz and 1.5 Hz, 1H), 2.87 (t, J = 6.9 Hz, 2H), 2.27 (t, J = 7.3 Hz, 2H), 1.68 (p, J = 7.1 Hz, 2H). ^{13}C NMR (MeOD-d^6, 63 MHz): δ = 177.01, 155.48, 142.99, 142.44, 141.66, 130.71, 128.56 (q, $^2J_{CF}$ = 33.2 Hz), 125.87 (q, $^1J_{CF}$ = 270.7 Hz), 125.84, 123.62, 121.72, 119.58, 118.12, 115.51 (q, $^3J_{CF}$ = 4.0 Hz), 114.12 (q, $^3J_{CF}$ = 3.9 Hz), 43.42, 31.84, 26.08; LC/MS (ESI): 459.1 [M − H]$^-$, 461.8 [M+H]$^+$; HRMS (TOF, ESI-) cald for $C_{18}H_{18}N_4O_5F_3S$ [M − H]$^-$ 459.0950, found 459.0954; beige solid. Yield = 60%.

4.2.3.5. 3-{[4-({[2-amino-4-(trifluoromethyl)phenyl]carbamoyl}amino)benzenesulfonamido]methyl}benzoic acid **27**.

Chromatography on silica gel was eluting with CH_2Cl_2-MeOH (95:5 to 90:10). ^{1}H NMR (MeOD-d^6, 400 MHz): δ = 10.70 (bs, 1H), 9.47 (bs, 1H), 8.87 (t, J = 6.3 Hz, 1H), 8.71 (s, 1H), 8.63 (d, J = 7.6 Hz, 1H), 8.57–8.52 (m, 3H), 8.47 (d, J = 8.7 Hz, 2H), 8.27 (d, J = 7.6 Hz, 1H), 8.21 (t, J = 7.5 Hz, 1H), 7.87 (bs, 1H), 7.71 (bd, J = 8.4 Hz, 1H), 6.19 (bs, 2H), 4.83 (d, J = 6.3 Hz, 2H). ^{13}C NMR (MeOD-d^6, 101 MHz): δ = 173.85, 153.88, 144.95, 141.64, 139.53, 134.03, 132.80, 129.59, 129.57 (q, $^2J_{CF}$ = 34.4 Hz), 129.32, 129.09, 127.28, 124.20 (q, $^1J_{CF}$ = 271.9 Hz), 125.24, 124.58, 123.59, 118.76, 114.27 (q, $^3J_{CF}$ = 3.7 Hz), 112.85 (q, $^3J_{CF}$ = 4.1 Hz), 47.08.; LC/MS (ESI): 507.1 [M − H]$^-$, 508.8 [M+H]$^+$; HRMS (TOF, ESI-) cald for $C_{22}H_{18}N_4O_5F_3S$ [M − H]$^-$ 507.0950, found 507.0953; beige solid. Yield = 35%.

4.2.3.6. 3-[2-amino-4-(trifluoromethyl)phenyl]-1-(4-{[(1-methylpyrrolidin-3-yl)methyl]sulfamoyl}phenyl)urea **28**.

Chromatography on aluminum oxide gel was eluting with CH_2Cl_2-MeOH (90:10 to 85:15).

^{1}H NMR (MeOD-d^6, 250 MHz): δ = 7.66 (d, J = 9.0 Hz, 2H), 7.56 (d, J = 9.0 Hz, 2H), 7.43 (d, J = 7.7 Hz, 1H), 7.01 (d, J = 1.8 Hz, 1H), 6.86 (dd, J = 8.3 Hz and 1.4 Hz, 1H), 2.73 (d, J = 6.9 Hz, 2H), 2.66–2.59 (m, 1H), 2.57–2.46 (m, 2H), 2.34–2.17 (m, 2H), 2.28 (s, 3H), 1.95–1.79 (m, 1H), 1.41 (dt, J = 13.7 Hz and 7.0 Hz, 1H). ^{13}C NMR (MeOD-d^6, 63 MHz): δ = 153.49, 143.27, 141.31, 133.03, 127.52, 127.07, 126.91 (q, $^2J_{CF}$ = 32.0 Hz), 124.18 (q, $^1J_{CF}$ = 270.8 Hz), 124.10, 117.71, 113.80 (q, $^3J_{CF}$ = 4.0 Hz), 112.45 (q, $^3J_{CF}$ = 3.9 Hz), 58.97, 55.04, 48.18, 40.46, 37.45, 27.89; LC/MS (ESI): 470.0 [M − H]$^-$, 472.0 [M+H]$^+$; HRMS (TOF, ESI-) cald for $C_{20}H_{23}N_5O_3F_3S$ [M − H]$^-$ 470.1474, found 470.1479; white powder. Yield = 27%.

4.2.4. General procedure for synthesis of nitro-sulfonamide ester derivatives **30**–**31**

Into a round bottom flask within respective urea derivative **16** (1 eq, 1.48 mmol), phosphorous chloride (30 eq, 44.40 mmol) was added slowly at 0 °C under argon atmosphere. The reaction mixture was stirred at 60 °C for at least 3 h. After completion, phosphorous chloride was evaporated *in vacuo* and quenched adding cold water dropwise. The precipitate was filtrated and the residue was rinsed with cold water to give the corresponding sulfonyl chloride

derivative **29**; LC/MS (ESI): 422.3 $[M-H]^-$; light yellow solid.

To a solution of 3-hydroxyphenyl acetic acid (2 eq, 1.18 mmol) in dry dichloromethane, DMAP (0.5 eq, 0.3 mmol) and triethylamine (6 eq, 3.54 mmol) were added under argon atmosphere. Mixture was stirred at least 20 min at room temperature. Then, a solution of crude sulfonyl chloride **29** in dry dichloromethane was added dropwise at 0 °C. The reaction mixture was stirred overnight under argon atmosphere at room temperature. After completion, mixture was washed twice with 1 N HCl, once with water, once with brine, dried over Na_2SO_4, and evaporated *in vacuo* to afford a crude residue which was purified by flash column chromatography eluting with dichloromethane-methanol (97:2.5 to 90:10) to give compounds **30** and **31**.

*4.2.4.1. 2-(3-{[4-({[2-nitro-4-(trifluoromethyl)phenyl]carbamoyl}amino)benzenesulfonyl]oxy}phenyl)acetic acid **30**.* ^{1}H NMR (MeOD-d^6, 250 MHz): δ = 8.79 (d, J = 8.8 Hz, 1H), 8.45 (d, J = 1.5 Hz, 1H), 7.91 (dd, J = 9.1 Hz and 1.9 Hz, 1H), 7.70 (bs, 4H), 7.22 (t, J = 7.7 Hz, 1H), 7.15 (dt, J = 7.6 Hz and 1.3 Hz, 1H), 6.94–6.91 (m, 1H), 6.84 (ddd, J = 7.8 Hz, 2.3 Hz and 1.4 Hz, 1H), 3.52 (s, 2H). ^{13}C NMR (MeOD-d^6, 101 MHz): δ = 167.91, 151.58, 149.76, 144.83, 138.41, 136.96, 136.19, 131.01 (q, $^3J_{CF}$ = 3.3 Hz), 129.63, 129.22, 128.30, 127.95, 123.21 (q, $^1J_{CF}$ = 280.02 Hz), 123.17 (q, $^2J_{CF}$ = 34.5 Hz), 123.00, 122.88, 122.60, 120.43, 118.26, 40.04. LC/MS (ESI): 537.9 $[M-H]^-$, 540.0 $[M+H]^+$; HRMS (TOF, ESI-) cald for $C_{22}H_{15}N_3O_8F_3S$ $[M-H]^-$ 538.0532, found 538.0538; yellow foam. Yield = 38%.

*4.2.4.2. 2-(3-{[2-(3-{[4-({[2-nitro-4-(trifluoromethyl)phenyl]carbamoyl}amino)benzenesulfonyl]oxy}phenyl)acetyl]oxy}phenyl)acetic acid **31**.* ^{1}H NMR (MeOD-d^6, 250 MHz): δ = 8.73 (d, J = 9.0 Hz, 1H), 8.40 (d, J = 1.3 Hz, 1H), 7.85 (dd, J = 9.3 Hz and 2.0 Hz, 1H), 7.63 (d, J = 9.3 Hz, 2H), 7.59 (d, J = 9.3 Hz, 2H), 7.33–7.13 (m, 3H), 7.03 (d, J = 7.7 Hz, 1H), 6.98–6.88 (m, 3H), 6.88–6.81 (m, 1H), 3.76 (s, 2H), 3.54 (s, 2H). LC/MS(ESI): 672.8 $[M-H]^-$, 673.2 $[M]^-$, yellow foam. Yield = 16%.

*4.2.5. General procedure for synthesis of aniline-sulfone ester derivatives **32**–**33***

To a solution of pure nitro-sulfone ester derivative **30** and **31** (1 eq) in AcOEt, Tin(II) chloride was added (6 eq). The reaction mixture was refluxed during 2–8 h. After completion, saturated solution of Na_2CO_3 was added dropwise until pH 7–8. Then, the organic layer was extracted with ethyl acetate and washed once with water, once with brine, dried over Na_2SO_4, and evaporated *in vacuo* to afford a crude residue which was purified by flash column chromatography on silica gel was eluting with CH_2Cl_2-MeOH (95:5 to 90:10) to give compounds **32** and **33**, respectively.

*4.2.5.1. 2-(3-{[4-({[2-amino-4-(trifluoromethyl)phenyl]carbamoyl}amino)benzenesulfonyl]oxy}phenyl)acetic acid **32**.* ^{1}H NMR (DMSO-d_6, 250 MHz): δ = 11.94 (bs, 1H), 10.45 (bs, 1H), 7.83–7.60 (m, 5H), 7.31–7.16 (m, 2H), 7.06–6.97 (m, 2H), 6.84 (dd, J = 8.4 Hz and 1.4 Hz, 1H), 6.72 (dt, J = 7.4 Hz and 2.0 Hz, 1H), 5.60 (bs, 2H), 3.41 (s, 2H). ^{13}C NMR (DMSO-d_6, 101 MHz): δ = 175.25, 153.65, 149.43, 147.46, 140.99, 140.94, 129.84, 129.57, 128.64, 128.54, 125.60, 125.21 (q, $^1J_{CF}$ = 271.3 Hz), 124.31 (q, $^2J_{CF}$ = 31.3 Hz), 123.23, 123.19, 119.65, 117.86, 112.71 (q, $^3J_{CF}$ = 3.8 Hz), 111.96 (q, $^3J_{CF}$ = 3.7 Hz), 44.21. LC/MS (ESI): 508.1 $[M-H]^-$, 510.8 $[M+H]^+$; HRMS (TOF, ESI-) cald for $C_{22}H_{17}N_3O_6F_3S$ $[M-H]^-$ 508.0790, found 508.0796; light yellow solid. Yield = 73%.

*4.2.5.2. 2-(3-{[2-(3-{[4-({[2-amino-4-(trifluoromethyl)phenyl]carbamoyl}amino)benzenesulfonyl]oxy}phenyl)acetyl]oxy}phenyl)acetic acid **33**.* ^{1}H NMR (DMSO-d_6, 400 MHz): δ = 10.73 (bs, 1H), 9.30 (bs, 1H), 7.73–7.65 (m, 4H), 7.39 (t, J = 7.8 Hz, 1H), 7.35–7.30 (m, 2H), 7.13 (d, J = 7.6 Hz, 1H), 7.09–7.02 (m, 4H), 6.96 (bd, J = 8.0 Hz, 1H), 6.87 (bd, J = 8.3 Hz, 1H), 3.97 (s, 2H), 3.53 (s, 2H). ^{13}C NMR (DMSO-d_6, 101 MHz): δ = 169.95, 153.15, 150.79, 149.71, 146.77, 141.09, 136.51, 130.38, 130.15, 129.53, 129.08, 128.35, 128.33, 127.46, 126.98, 125.88, 125.12 (q, $^1J_{CF}$ = 271.1 Hz), 124.36 (q, $^2J_{CF}$ = 38.9 Hz), 123.52, 123.16, 122.69, 121.49, 119.80, 117.89, 113.19 (q, $^3J_{CF}$ = 3.8 Hz), 111.97 (q, $^3J_{CF}$ = 3.7 Hz) 42.68, 39.96. LC/MS (ESI): 642.1 $[M-H]^-$, 644.9 $[M+H]^+$; HRMS (TOF, ESI-) cald for $C_{30}H_{23}N_3O_8F_3S$ $[M-H]^-$ 642.1158, found 642.1160; white powder. Yield = 53%.

4.3. DENV and ZIKV 2′-O-MTase inhibition testing and data analysis

The coding sequence of the ZIKV MTase domain was cloned in pDest 14 expression vector as recently described [21], and the corresponding protein was produced and purified following the protocols previously applied for the DENV MTase [35].

DENV-3 and ZIKV 2′-*O*-MTase activity was assayed by incubating the corresponding MTase with a selected fragment and a small capped RNA substrate $GpppAC_4$ in the presence of [^{3}H]AdoMet [40,41]. The MTase activity assay was performed in 20 μL samples containing 40 mM Tris-HCl pH 7.5, 5 mM DTT, 10 μM AdoMet (0.2–2 μCi [^{3}H]AdoMet), 1 μM of MTase, 0.5–2 mM of fragment (stock solutions 100 mM in 100% DMSO) and 1 μM $GpppAC_4$. The enzyme, buffer and fragments were first mixed together and the reaction was started by adding a premix of AdoMet and capped RNA substrates. Reactions were incubated at 30 °C for 30 min and stopped by 20-fold dilution in an ice-cold 100 μM AdoHcy solution. Samples were then transferred onto a DEAE membrane (DEAE Filtermat; Wallac) by a Filtermat Harvester (Packard Instruments) washed with 0.01 M ammonium formate (pH 8.0), water and ethanol, and the radioactivity transferred onto RNA was measured using a Wallac 1450 MicroBeta Trilux Liquid Scintillation Counter [35].

The inhibitor concentration at 50% activity (IC_{50}) was determined by performing DENV-3 and ZIKV MTase assays as described in presence of a serial dilution of the inhibitor. MTase assays were performed as described above. The final concentration of DMSO in reaction mixtures was below 5%. All data points were measured in duplicate. The IC_{50} values were determined using Prism software and adjusted to a logistic dose-response function: % activity = $100/(1+[I]/IC_{50})^b$, where b corresponds to the slope factor and [I] to inhibitor concentration [42].

Acknowledgements

We wish to thank Manon Garcia and Sarah Attoumani for technical assistance. This work was supported by the European program H2020 under the ZIKAlliance project (grant agreement 734548), the EVAg Research Infrastructure (grant agreement 653316) and by the French research agency ANR (VMTaseIn, grant ANR-ST14-ASTR-0026, and FragVir, grant ANR-13-JS07-0006-01).

Appendix A. Supplementary data

Supplementary data to this article can be found online at https://doi.org/10.1016/j.ejmech.2018.09.056.

References

[1] W.L. Walker, N.P. Lindsey, J.A. Lehman, E.R. Krow-Lucal, I.B. Rabe, S.L. Hills, S.W. Martin, M. Fischer, J.E. Staples, Zika Virus Disease Cases-50 States and the District of Columbia, January 1-July 31, 2016, vol. 65, Mmwr-Morbid Mortal W, 2016, pp. 983–986.

[2] C.V. Ventura, M. Maia, V. Bravo-Filho, A.L. Gois, R. Belfort, Zika virus in Brazil and macular atrophy in a child with microcephaly, Lancet 387 (2016), 228-228.

[3] V.M. Cao-Lormeau, A. Blake, S. Mons, S. Lastere, C. Roche, J. Vanhomwegen, T. Dub, L. Baudouin, A. Teissier, P. Larre, A.L. Vial, C. Decam, V. Choumet, S.K. Halstead, H.J. Willison, L. Musset, J.C. Manuguerra, P. Despres, E. Fournier, H.P. Mallet, D. Musso, A. Fontanet, J. Neil, F. Ghawche, Guillain-Barre Syndrome outbreak associated with Zika virus infection in French Polynesia: a case-control study, Lancet 387 (2016) 1531–1539.
[4] T.J. Chambers, C.S. Hahn, R. Galler, C.M. Rice, Flavivirus genome organization, expression, and replication, Annu. Rev. Microbiol. 44 (1990) 649–688.
[5] E. Decroly, F. Ferron, J. Lescar, B. Canard, Conventional and unconventional mechanisms for capping viral mRNA, Nat. Rev. Microbiol. 10 (2012) 51–65.
[6] M. Bollati, K. Alvarez, R. Assenberg, C. Baronti, B. Canard, S. Cook, B. Coutard, E. Decroly, X. de Lamballerie, E.A. Gould, G. Grard, J.M. Grimes, R. Hilgenfeld, A.M. Jansson, H. Malet, E.J. Mancini, E. Mastrangelo, A. Mattevi, M. Milani, G. Moureau, J. Neyts, R.J. Owens, J. Ren, B. Selisko, S. Speroni, H. Steuber, D.I. Stuart, T. Unge, M. Bolognesi, Structure and functionality in flavivirus NS-proteins: perspectives for drug design, Antivir. Res. 87 (2010) 125–148.
[7] M.P. Egloff, D. Benarroch, B. Selisko, J.L. Romette, B. Canard, An RNA cap (nucleoside-2'-O-)-methyltransferase in the flavivirus RNA polymerase NS5: crystal structure and functional characterization, EMBO J. 21 (2002) 2757–2768.
[8] Y.S. Zhou, D. Ray, Y.W. Zhao, H.P. Dong, S.P. Ren, Z. Li, Y. Guo, K.A. Bernard, P.Y. Shi, H.M. Li, Structure and function of flavivirus NS5 methyltransferase, J. Virol. 81 (2007) 3891–3903.
[9] B.X. Wang, S. Thurmond, R. Hai, J.K. Song, Structure and function of Zika virus NS5 protein: perspectives for drug design, Cell. Mol. Life Sci. 75 (2018) 1723–1736.
[10] H.P. Dong, D.C. Chang, X.P. Xie, Y.X. Toh, K.Y. Chung, G. Zou, J. Lescar, S.P. Lim, P.Y. Shi, Biochemical and genetic characterization of dengue virus methyltransferase, Virology 405 (2010) 568–578.
[11] R. Zust, L. Cervantes-Barragan, M. Habjan, R. Maier, B.W. Neuman, J. Ziebuhr, K.J. Szretter, S.C. Baker, W. Barchet, M.S. Diamond, S.G. Siddell, B. Ludewig, V. Thiel, Ribose 2'-O-methylation provides a molecular signature for the distinction of self and non-self mRNA dependent on the RNA sensor Mda5, Nat. Immunol. 12 (2011) 137–143.
[12] R. Zust, H. Dong, X.F. Li, D.C. Chang, B. Zhang, T. Balakrishnan, Y.X. Toh, T. Jiang, S.H. Li, Y.Q. Deng, B.R. Ellis, E.M. Ellis, M. Poidinger, F. Zolezzi, C.F. Qin, P.Y. Shi, K. Fink, Rational design of a live attenuated dengue vaccine: 2'-o-methyltransferase mutants are highly attenuated and immunogenic in mice and macaques, PLoS Pathog. 9 (2013) e1003521.
[13] S.H. Li, H.P. Dong, X.F. Li, X.P. Xie, H. Zhao, Y.Q. Deng, X.Y. Wang, Q. Ye, S.Y. Zhu, H.J. Wang, B. Zhang, Q.B. Leng, R. Zuest, E.D. Qin, C.F. Qin, P.Y. Shi, Rational design of a flavivirus vaccine by abolishing viral RNA 2 '-O methylation, J. Virol. 87 (2013) 5812–5819.
[14] S.P. Lim, L.S. Sonntag, C. Noble, S.H. Nilar, R.H. Ng, G. Zou, P. Monaghan, K.Y. Chung, H.P. Dong, B.P. Liu, C. Bodenreider, G. Lee, M. Ding, W.L. Chan, G. Wang, Y.L. Jian, A.T. Chao, J. Lescar, Z. Yin, T.R. Vedananda, T.H. Keller, P.Y. Shi, Small molecule inhibitors that selectively block dengue virus methyltransferase, J. Biol. Chem. 286 (2011) 6233–6240.
[15] M. Brecher, H. Chen, B.B. Liu, N.K. Banavali, S.A. Jones, J. Zhang, Z. Li, L.D. Kramer, H.M. Li, Novel broad spectrum inhibitors targeting the flavivirus methyltransferase, PloS One 10 (2015).
[16] P. Stephen, M. Baz, G. Boivin, S.X. Lin, Structural insight into NS5 of Zika virus leading to the discovery of MTase inhibitors, J. Am. Chem. Soc. 138 (2016) 16212–16215.
[17] R. Jain, K.V. Butler, J. Coloma, J. Jin, A.K. Aggarwal, Development of a S-adenosylmethionine analog that intrudes the RNA-cap binding site of Zika methyltransferase, Sci Rep-Uk 7 (2017).
[18] S.P. Lim, Q.Y. Wang, C.G. Noble, Y.L. Chen, H. Dong, B. Zou, F. Yokokawa, S. Nilar, P. Smith, D. Beer, J. Lescar, P.Y. Shi, Ten years of dengue drug discovery: progress and prospects, Antivir. Res. 100 (2013) 500–519.
[19] B. Coutard, E. Decroly, C.Q. Li, A. Sharff, J. Lescar, G. Bricogne, K. Barral, Assessment of Dengue virus helicase and methyltransferase as targets for fragment-based drug discovery, Antivir. Res. 106 (2014) 61–70.
[20] F. Benmansour, I. Trist, B. Coutard, E. Decroly, G. Querat, A. Brancale, K. Barral, Discovery of novel dengue virus NS5 methyltransferase non-nucleoside inhibitors by fragment-based drug design, Eur. J. Med. Chem. 125 (2017) 865–880.
[21] B. Coutard, K. Barral, J. Lichiere, B. Selisko, B. Martin, W. Aouadi, M.O. Lombardia, F. Debart, J.J. Vasseur, J.C. Guillemot, B. Canard, E. Decroly, Zika virus methyltransferase: structure and functions for drug design perspectives, J. Virol. 91 (2017).
[22] M. Hartenfeller, M. Eberle, P. Meier, C. Nieto-Oberhuber, K.H. Altmann, G. Schneider, E. Jacoby, S. Renner, A collection of robust organic synthesis reactions for in silico molecule design, J. Chem. Inf. Model. 51 (2011) 3093–3098.
[23] L. Hoffer, J.P. Renaud, D. Horvath, In silico fragment-based drug discovery: setup and validation of a fragment-to-lead computational protocol using S4MPLE, J. Chem. Inf. Model. 53 (2013) 836–851.
[24] L. Hoffer, C. Chira, G. Marcou, A. Varnek, D. Horvath, S4MPLE-Sampler for multiple protein-ligand entities: methodology and rigid-site docking benchmarking, Molecules 20 (2015) 8997–9028.
[25] D.A. Jose, D.K. Kumar, P. Kar, S. Verma, A. Ghosh, B. Ganguly, H.N. Ghosh, A. Das, Role of positional isomers on receptor-anion binding and evidence for resonance energy transfer, Tetrahedron 63 (2007) 12007–12014.
[26] J. Valgeirsson, E.O. Nielsen, D. Peters, C. Mathiesen, A.S. Kristensen, U. Madsen, Bioisosteric modifications of 2-arylureidobenzoic acids: selective noncompetitive antagonists for the homomeric kainate receptor subtype GluR5, J. Med. Chem. 47 (2004) 6948–6957.
[27] Z.G. Li, H. Huang, H.B. Sun, H.L. Hang, H. Liu, Microwave-assisted efficient and convenient synthesis of 2,4(1H,3H)-quinazolinediones and 2-thioxoquinazolines, J. Comb. Chem. 10 (2008) 484–486.
[28] J. Azizian, A.A. Mohammadi, A.R. Karimi, An efficient one-pot procedure for preparation of 2,4(1H,3H)-qninazolinediones and 2-thioxoquinazolinone derivatives under microwave irradiation, Synth. Commun. 33 (2003) 415–420.
[29] F.D. Bellamy, K. Ou, Selective reduction of aromatic nitro-compounds with stannous chloride in non-acidic and non-aqueous medium, Tetrahedron Lett. 25 (1984) 839–842.
[30] K. Ghosh, I. Saha, Triphenylamine-based simple chemosensor for selective fluorometric detection of fluoride, acetate and dihydrogenphosphate ions in different solvents, J Incl Phenom Macro 70 (2011) 97–107.
[31] N. Abbassi, E. Rakib, A. Hannioui, M. Alaoui, M. Benchidmi, E. Essassi, D. Geffken, Alkylation and reduction of N-alkyl-4-nitroindazoles with anhydrous SnCl2 in ethanol: synthesis of novel 7-ethoxy-N-alkylindazole derivatives, Heterocycles 83 (2011) 891–900.
[32] H. Venkatesan, F.M. Hocutt, T.K. Jones, M.H. Rabinowitz, A one-step synthesis of 2,4-unsubstituted quinoline-3-carboxylic acid esters from o-nitrobenzaldehydes, J. Org. Chem. 75 (2010) 3488–3491.
[33] R. Ding, Y. He, X. Wang, J.L. Xu, Y.R. Chen, M. Feng, C.M. Qi, Treatment of alcohols with tosyl chloride does not always lead to the formation of tosylates, Molecules 16 (2011) 5665–5673.
[34] K. Katakawa, D. Yonenaga, T. Terada, N. Aida, A. Sakamoto, K. Hoshino, T. Kumamoto, Selective synthesis of benzyl enol ethers of beta-dicarbonyl compounds in basic condition and the application towards synthesis of naphthoquinones, Heterocycles 88 (2014) 817–825.
[35] K. Barral, C. Sallamand, C. Petzold, B. Coutard, A. Collet, Y. Thillier, J. Zimmermann, J.J. Vasseur, B. Canard, J. Rohayem, F. Debart, E. Decroly, Development of specific dengue virus 2'-O- and N7-methyltransferase assays for antiviral drug screening, Antivir. Res. 99 (2013) 292–300.
[36] F. Benmansour, C. Eydoux, G. Querat, X. de Lamballerie, B. Canard, K. Alvarez, J.C. Guillemot, K. Barral, Novel 2-phenyl-5-[(E)-2-(thiophen-2-yl)ethenyl]-1,3,4-oxadiazole and 3-phenyl-5-[(E)-2-(thiophen-2-yl)ethenyl]-1,2,4-oxadiazole derivatives as dengue virus inhibitors targeting NS5 polymerase, Eur. J. Med. Chem. 109 (2016) 146–156.
[37] J. Kazius, R. McGuire, R. Bursi, Derivation and validation of toxicophores for mutagenicity prediction, J. Med. Chem. 48 (2005) 312–320.
[38] J. Coloma, R. Jain, K.R. Rajashankar, A. Garcia-Sastre, A.K. Aggarwal, Structures of NS5 methyltransferase from Zika virus, Cell Rep. 16 (2016) 3097–3102.
[39] G.W. Bemis, M.A. Murcko, The properties of known drugs .1. Molecular frameworks, J. Med. Chem. 39 (1996) 2887–2893.
[40] M. Milani, E. Mastrangelo, M. Bollati, B. Selisko, E. Decroly, M. Bouvet, B. Canard, M. Bolognesi, Flaviviral methyltransferase/RNA interaction: structural basis for enzyme inhibition, Antivir. Res. 83 (2009) 28–34.
[41] B. Selisko, F.F. Peyrane, B. Canard, K. Alvarez, E. Decroly, Biochemical characterization of the (nucleoside-2'O)-methyltransferase activity of dengue virus protein NS5 using purified capped RNA oligonucleotides (7Me)GpppAC(n) and GpppAC(n), J. Gen. Virol. 91 (2010) 112–121.
[42] A. Delean, P.J. Munson, D. Rodbard, Simultaneous analysis of families of sigmoidal curves - application to bioassay, radioligand assay, and physiological dose-response curves, Am. J. Physiol. 235 (1978) E97–E102.